Rover Localization and Landing-Site Mapping Technology for the 2003 Mars Exploration Rover Mission

Rongxing Li, Kaichang Di, Larry H. Matthies, Raymond E. Arvidson, William M. Folkner, and Brent A. Archinal

Abstract

The technology and experiments planned for rover localization and landing site mapping in the 2003 Mars Exploration Rover (MER) mission are described. We introduce the Mars global and landing site local reference systems. For global rover localization in the Mars body-fixed reference system, a triangulation can be performed using observations of common landmarks on satellite images and the very first set of surface images. Alternatively, ultra-high frequency (UHF) two-way Doppler tracking technology can determine the location. For localization of the rover in the landing site area, onboard rover localization techniques will be performed in real time. A visual odometry experiment will improve localization by overcoming problems associated with wheel odometry such as slippage and low accuracy. Finally, a bundle-adjustment-based rover localization method will build an image network acquired by Pancam, Navcam, and Hazcam cameras. The developed incremental and integrated bundle adjustment models will supply improved rover locations and image orientation parameters, which are critical for the generation of high quality landing site topographic mapping products. Based on field tests performed on Earth and Mars (MPF mission data), a relative localization accuracy of one percent of the traversing distance from the landing center is expected to be achieved during this mission. In addition, the bundle adjustment results will also enable us to produce high precision landing site topographic mapping products, including seamless panoramic image mosaics, DTMs, and orthophotos.

Introduction

The science objectives of the National Aeronautics and Space Administration (NASA) Mars Exploration Program focus on understanding the current and past habitability of Mars on a global scale. This means understanding the spatial and temporal patterns associated with tectonic and hydrologic cycles that have operated on and within Mars, and how these processes have modulated geochemical cycles of possible biological relevance. Measurements have been and/or will continue to be made from orbital platforms such as the Mars Global Surveyor (MGS) (URL: http://mars.jpl.nasa.gov/mgs/, last accessed 06 October 2003), Mars Odyssey (URL: http://mars.jpl.nasa.gov/odyssey/, last accessed 06 October 2003), and 2005 Mars Reconnaissance Orbiter (URL: http://mars.jpl.nasa.gov/missions/future/2005-plus.html, last accessed 06 October 2003). Efforts will focus, in part, on mapping in detail those locations that would be prime targets for detailed surface exploration and return sample missions. In particular, mapping would include delineation of morphology, topography, mineralogy, and elemental abundances using an array of instrumentation. Sites of interest include locations where ancient seas, lakes, or river systems are thought to have left behind a sedimentary rock record, and areas that are inferred to be extant or ancient hydrothermal zones and associated deposits. These locations would be excellent targets for rover missions that would explore laterally and make measurements that would complement orbital observations and allow testing of hypotheses developed from orbital data and other observations. The focus will be on reaching and exploring sedimentary and hydrothermal deposits because these materials may preserve evidence needed to decipher past environmental conditions. Perhaps they may even hold biosignatures.

Before the U.S. lander missions, the Soviet Union had attempted five landings on Mars, none of which were successful. The first U.S. mission with such a ground observation capability was the Viking Lander Mission in 1976, which acquired Martian surface images using its lander imagers (Binder *et al.*, 1977; Mutch *et al.*, 1977). The Mars Pathfinder (MPF) mission sent the Sojourner rover equipped with a suite of observation tools to the Martian surface for traversing and exploring a landing site of about 10 m by 10 m in 1997 (Golombek, 1997; Golombek *et al.*, 1999). In 2003, the Mars Exploration Rover (MER) mission has successfully launched two larger and better-equipped rovers, named Spirit and Opportunity, that will land on two different sites (Gusev and Meridiani) on Mars (Squyres *et al.*, 2004; Crisp *et al.*, 2004). The two rovers will document the geology of the landing sites and gather compositional, mineralogical, and textural information about selected Martian soils and rocks. Having far greater mobility, the MER rovers will be able to travel up to 100 meters across the surface each Martian day. The cumulative distance traversed by the rover is

R. Li and K. Di are with the Department of Civil and Environmental Engineering and Geodetic Science, The Ohio State University, 470 Hitchcock Hall, 2070 Neil Avenue, Columbus, OH 43210 (li.282@osu.edu).

L.H. Matthies is at Mail Stop 125-209 and W.M. Folkner is at Mail Stop 238-116, both at the Jet Propulsion Laboratory, 4800 Oak Grove Drive, Pasadena, CA 91109.

R.E. Arvidson is with the Department of Earth and Planetary Sciences, McDonnell Center for the Space Sciences, Washington University, One Brookings Drive, Campus Box 1169, St. Louis, MO 63130.

B.A. Archinal is with the U.S. Geological Survey, 2255 N. Gemini Drive, Flagstaff, AZ 86001.

Photogrammetric Engineering & Remote Sensing
Vol. 70, No. 1, January 2004, pp. 77–90.

0099-1112/04/7001–0077/$3.00/0
© 2004 American Society for Photogrammetry and Remote Sensing

Figure 1. Simulated image of MER 2003 rover.

planned for 600 m to 1,000 m (URL: http://mars.jpl.nasa.gov/missions/future/2003.html, last accessed 06 October 2003).

The two MER rovers (Figure 1) are identical and each carries an identical Athena Instrument Payload and engineering cameras (Squyres *et al.*, 2004). Table 1 lists the MER rover sensors and key parameters. We discuss the ones that are relevant to the experiments depicted in this paper. Each rover is a six-wheel drive, four-wheel steered vehicle with a rocker-bogie suspension system similar in design to the Sojourner rover. The vehicles are designed with a ground clearance of 0.3 m and the rover rocker-bogie design allows for traversing obstacles of more than a wheel diameter (25 cm) in size. Each rover carries an inertial measurement unit (IMU) that provides three-axis rate and three-axis tilt information. The rover automatically estimates its position using wheel odometry and IMU data. Among the various instruments, Pancam (Panoramic Camera) and Navcam (Navigation Camera) are the most important ones for detailed landing site mapping and rover localization. These two stereo imaging systems are mounted on the same bar of the rover mast. Pancam has a longer base of 30 cm and a longer focal length of 38 mm, making it more effective in mapping medium to far objects in the panoramic images. The imaging areas of both Pancam and Navcam are 1,024 by 1,024 pixels. The effective depth of field for the Pancam is 3 m to infinity and the field of view (FOV) is 16 degrees. The Navcam has a focal length of 14.67 mm and an effective depth of field from 0.5 m to infinity. Its best focus is at 1 m and the FOV is 45 degrees (Table 1).

Other cameras will include the Hazcams and the Microscopic Imager (MI). The Hazcams (Hazard-avoidance Cameras) are used to determine safe egress directions for the rover and provide for onboard hazard detection using stereo data to build range maps. Two pairs of Hazcams are mounted on the front and rear end of the rovers' warm electronics boxes below the solar panel. Each Hazcam assembly includes two cameras that form a 10-cm stereo baseline. The FOV is approximately 120 degrees and the depth of field is 0.1 m to infinity. The focal length is 5.58 mm, and the best focus is at 0.4 m. The Microscopic Imager is a 1024- by 1024-pixel imaging system mounted on an extendable arm (the Instrument Deployment Device, or IDD). The focal length is 20 mm. It has a fixed focus design that provides a 31- by 31-mm field of view at a 30 μm per pixel resolution, at a distance of 63 mm from the lens, with a depth of field of ± 3 mm. It will provide extreme close-ups of rock and soil samples, which must be localized within the images of the other cameras.

TABLE 1. MER ROVER SENSORS AND KEY PARAMETERS

Instrument	Key Parameters
Mast-Mounted	
Pancam: Panoramic Camera	Twelve bands (0.4 to 1.0 μm) for stereoscopic imaging with 0.28-mrad IFOV; 16.8-deg by 16.8-deg FOV. Stereobaseline separation of 30 cm. External calibration target on rover deck.
Mini-TES: Thermal Emission Spectrometer	Emission spectra (5 to 29 μm, 10-cm resolution) with 8- or 20-mrad FOV. Internal and external blackbody calibration targets.
IDD-Mounted *In-Situ* Package	
APXS: Alpha Particle X-Ray Spectrometer	Cm alpha particle sources, and x-ray detectors, 3.8-cm FOV.
MB: Mössbauer Spectrometer	Fe spectrometer in backscatter mode; Co/Rh source and Si-PIN diode detectors; field of view approximately 1.5 cm^2.
MI: Microscopic Imager	30-μm/pixel monochromatic imager (1024 by 1024) with 6-mm depth of field.
RAT: Rock Abrasion Tool	Tool capable of preparing 5-mm deep by 4.5-cm wide surface on rocks.
Magnets	
Filter	Located front of rover within Pancam FOV. Weak magnet to cull suspended particles from atmosphere.
Capture	Located front of rover within Pancam FOV next to Capture Magnet. Strong magnet to cull suspended particles from atmosphere.
Sweep	Located next to Pancam calibration target. Intended to separate magnetic from non magnetic particles. To be examined by Pancam.
RAT	Four magnets of different strengths in RAT. To be examined by Pancam when IDD points RAT toward cameras.
Engineering Cameras	
Navigation Cameras (Navcam)	Mast-mounted panchromatic stereoscopic imaging system with 0.77-mrad IFOV; 45-deg FOV, and 20-cm stereobaseline separation. For planning sequences.
Hazard Avoidance Cameras (Hazcam)	Front and rear-looking panchromatic stereoscopic imaging systems with 2-mrad IFOV; 123-deg FOV, 10-cm stereobaseline separation. For path planning and hazard avoidance during traverses.

Locational knowledge will be essential to the success of the 2003 MER mission, particularly to such goals as being able to define global locations of features on the ground, for example, channel deposits or volcanic vents. Such knowledge is also essential to being able to land on or adjacent to these features with some degree of precision. Precise locational knowledge will allow one to track the location of the two rovers in order to know where on Mars the observations were made and how they fit within sequences of observations acquired from an orbital perspective. To that end, the expectation is that the Mars Exploration rovers will use two-way radio tracking in order to define their location. It will also be important to be able to define the location of the landing site relative to terrain features observed in orbital images that have been taken by the Viking camera, MGS Mars Orbiter Camera (MOC), and Odyssey Thermal Emission Imaging System (THEMIS). This will be accomplished by cross-correlating features observed on ground images acquired from the rovers with features observed in the orbital images. Furthermore, we will need to determine where the rover has been as measured in local Cartesian coordinates by cross-correlating features observed in overlapping rover images. This information will be coupled with locational information derived from the orbital images, and the result will then be transformed into the global coordinate system. The overall key will be to be able to relate observations from orbit with those from the rovers in order to be able to test and update hypotheses related to planetary habitability. Locational knowledge is a crucial link in relating the sets of observations.

The onboard navigation system consists mainly of an IMU, an odometer, and solar imaging cameras (Pancam). The nominal rover localization error of this system is 10 percent of the traversing distance from the landing center. As planned for the MER mission, this may result in an error of 100 m accumulated over a traverse of 1,000 m. Thus, mapping products derived from the rover images could contain large errors. If not dealt with appropriately, these errors would significantly affect landing site operations when the rovers traverse areas farther away from the landing center.

The localization experiments of the MER mission will include global localization by matching common features in orbital and surface images and by radio tracking. Local rover localization on the landing site will be based on the onboard navigation sensors. However, improvement of the localization is expected by using an image-based rover localization approach that uses a network of surface images along with bundle adjustment techniques. This will enhance not only the localization accuracy, but also the topographic mapping quality.

There will be a number of groups involved in the rover localization and landing site mapping tasks in the MER mission. The U.S. Geological Survey (USGS) Astrogeology Team and members of the Mars Geodesy and Cartography Working Group (MGCWG) will produce cartographic maps of the landing sites using orbital data before the landing. They may process the data collected during the mission and produce accurate mapping products on a "longer term" basis during or after the mission. The Jet Propulsion Laboratory (JPL) radio tracking team will conduct rover localization through ultra high frequency (UHF) two-way Doppler tracking and provide the precise spacecraft location shortly after landing. The Pancam instrument team of Cornell University will operate the Pancam imaging system that collects high-resolution surface images for science and engineering experiments. Matching of the remote landmarks in orbital images and surface images will be performed by the Athena Science Team. The JPL rover engineering team is responsible for navigation operation using the onboard navigation system and software system on Earth. The JPL Multimission Image Processing Laboratory (MIPL) will produce image mosaics using the Video Image Communication and Retrieval (VICAR) image processing system to support rover navigation and operations. They will also supply some mapping products, including range maps using non-adjusted individual stereo images within a very short turnaround time (within a sol, i.e., a Martian day). The Science Activity Planner (SAP) system developed by the JPL Web Interface for Telescience (WITS) team will be an effective tool for the Athena science team members to use downlinked images, range maps, mosaics, and measuring functions for various science oriented operations. The photogrammetric bundle adjustment method and visual odometry method will be used by The Ohio State University (OSU) team and the JPL machine vision group to provide improved rover locations and mapping products within a sol or in several sols. The results will be used to support the science team experiments and to demonstrate the potential of this new technique for future long-range rover traversing, but they will not be used in rover engineering operations in this mission. The Earth and Planetary Remote Sensing Laboratory at Washington University in St. Louis will be responsible for using the localization results and mapping products for investigation of Martian surface physical properties and archiving the images and mapping products in the Planetary Data System (PDS) Geosciences node. This paper summarizes many of these activities. More details are given on visual odometry and image-network-based bundle adjustment for rover localization and landing site mapping.

Reference Systems

Mars Global Reference System

In this section, we discuss primarily two Mars-centered coordinate systems. One is an inertial system, which, for example, can be used to determine orbiting spacecraft coordinates. The other is a body-fixed system, which determines coordinates of surface features, landers, and rovers. The connection between the two systems defines the "rotation" of Mars.

Inertial Reference System

Coordinates in the Mars inertial reference system are derived entirely from tracking of spacecraft orbiting or on the surface of Mars. The origin of this system is the center of mass of Mars, as it has been determined from such spacecraft tracking. Its orientation is that of the International Celestial Reference System, defined in practice by the coordinates of distant radio sources (e.g., quasars) that make up the International Celestial Reference Frame, or ICRF (Ma *et al.*, 1998). Because the same radio telescopes that are used for spacecraft tracking can also observe these (or related) ICRF radio sources, spacecraft coordinates can be quite accurately located in this frame.

Mars Body-Fixed Reference System

The Mars body-fixed reference system is defined essentially by the International Astronomical Union/International Association of Geodesy (IAU/IAG) Working Group on Cartographic Coordinates and Rotational Elements of the Planets and Satellites in their most recent report (Seidelmann *et al.*, 2002). Two types of Mars fixed coordinate systems are allowed: (1) a spherical coordinate system using latitude (called planetocentric or areocentric) and longitude measured toward the east, and (2) an ellipsoidal coordinate system using planetographic latitude and longitude measured toward the west. In the latter system, the latitude is measured as the angle between the equatorial plane and the normal to the ellipsoidal reference surface at a given point. In either system, the rotational pole of Mars on the north side of the invariable plane of the solar system specifies the north direction and northern latitudes are measured as positive. Longitudes range from 0 to 360 degrees.

The origin for longitude on Mars is the center of the small crater Airy-0 with a diameter of about 500 m (de Vaucouleurs *et al.*, 1973). These specifications also imply that the geometrical center of either the spherical or the ellipsoidal system is the center of mass of Mars (as in the Mars inertial system).

Historically, the planetographic latitude and west longitude have most often been used in making maps of Mars. However, the Mars Orbiter Laser Altimeter (MOLA) Science Team adopted the use of planetocentric latitude and east longitude for their operational work and products. Due partly to the highest accuracy and detailed information provided by the MOLA products and their recent widespread use (Smith *et al.*, 2001; Duxbury *et al.*, 2002), the latter method of defining coordinates has come into widespread use. The MER mission has adopted the use of this system (Duxbury *et al.*, 2002) as has the Odyssey and Mars Reconnaissance Orbiter Missions.

Although not specifically discussed by the IAU/IAG Working Group, it is assumed that, in order to truly specify the coordinates of a feature on Mars in three dimensions, the planetary radius (e.g., in km or m) of that feature must be specified along with its planetocentric latitude and east longitude. Furthermore, coordinates in such a Mars body-fixed reference system may easily be converted to Cartesian coordinates. When expressed in these coordinates and with an origin at the Mars center of mass, the *X*-axis is then in the direction of the intersection of the Prime Meridian (which passes through the center of Airy-0) and it lies in the equatorial plane, the *Z*-axis is in the direction of the north pole, and the *Y*-axis forms a right-hand system with the other axes. Such a system obviously lends itself to various calculations and, in fact, it is in common use.

Rotation

As previously explained, the difference between the Mars inertial reference system and the body-fixed reference system is the "rotation," or orientation, of Mars. According to the IAU/IAG Working Group, it is defined by specifying that the north pole of the rotation axis of the Mars body-fixed reference system points to right ascension (α) and declination (δ): $\alpha = 317.68143° - 0.1061°$/century T and $\delta = 52.88650° - 0.0609°$/century T, of the ICRF, where T is the interval in Julian centuries (of 36525 days) from the standard epoch, i.e., J2000.0 = 2000 January 1.5 TDB (barycentric dynamical time). The orientation of Mars on its axis is defined by $W = W_0 + 350.89198226°$/day d, where W is the angle measured along the equator from the equator's intersection with the celestial equator to the Prime Meridian and d is the interval in days from the standard epoch. The fixed term W_0 is 176.630° and was recently redetermined by comparing MOLA-derived coordinates and digital image models with Viking and Mars Orbiter Camera (MOC) images of the Airy-0 crater. This work was undertaken by the NASA Mars Geodesy and Cartography Working Group and is reported in Duxbury *et al.* (2002). This new value was derived with an absolute accuracy of about ±250 m and has been adopted by the IAU/IAG Working Group along with a new determination for Mars's spin rate (Folkner *et al.*, 1997). From radio tracking of the Viking and Mars Pathfinder landers, Mars is actually known to have slight variations in its orientation from these values (Folkner *et al.*, 1997). However, they have not yet been measured (or at least modeled) at a level accurate enough to allow for their prediction.

Elevation

The "height" of features on Mars can be expressed as a radius, i.e., the distance from a feature to the Mars center of mass. For many purposes, it is also useful to specify the "elevation" of a given feature, such as some measure of the gravity potential at that feature relative to some standard average gravity potential for the surface of Mars. The surface having this standard gravity potential is known as the areoid, or Martian gravitational equipotential surface. In the past, definitions of the areoid and elevations on Mars were based on such data as radar and radio occultation measurements of Martian radii and stereo-derived height information as defined through work at the USGS (Wu, 1975) and elsewhere (see Smith *et al.* (2001, p. 23690) for a brief review). With accuracies commonly at the ±1-km level, these types of height measurements are now of historical information only, having been completely superseded by results from the MGS Mars Orbiter Laser Altimeter (MOLA) measurements. The MOLA measurements now define the topographic surface on Mars with an accuracy (in radius) at the 10-m level, a precision at the 1-m level, and a horizontal accuracy at the 100-m level (Neumann *et al.*, 2001). In addition, precise tracking of the MGS spacecraft carrying the MOLA instrument has allowed the gravity field of Mars to be determined at a level where the predicted error in areoidal heights ranges from 1.0 to 2.6 m, with a global root-mean-square error (RMSE) of 1.8 m (Lemoine *et al.*, 2001) and maximum uncertainties of about 10 to 20 m (Neumann, 2002). The areoid on Mars has been defined (Smith *et al.*, 2001, p. 23696) as the equipotential surface (of gravity, equal to gravitational plus rotational) whose average value at the equator is equal to the mean radius of the solid surface at the equator (or 3396.000 km as determined by MOLA). From the above-mentioned specifications and knowledge of the gravity field (Lemoine *et al.*, 2001), the elevation of all points on Mars can be computed. From the topographic information of the areoid at the level of precision cited above, the elevation will therefore have nearly the same 10-m absolute precision. This means that once the planetocentric latitude and east longitude of any surface feature or rover position are determined, a MOLA digital terrain model (DTM) for topography, expressed either as radius or elevation, can be interpolated to give those values. Because the MOLA data themselves have an absolute horizontal uncertainty of ±100 m, and because there will always be some additional uncertainty in determining the coordinates of any feature or rover position, the absolute accuracy of these values would be at least 10 m in areas of rough terrain or steep slopes. However, for the rovers, which are expected to land on relatively flat terrain, radius and elevation can be expected to be accurate to the 10-m level and to have precisions (e.g., for relative determination of elevation between nearby locations) even higher than this, perhaps limited only by the ±1-m precision of the MOLA topographic model. Currently, the MOLA science team is preparing a final version of the MOLA topographic model (in both radius and gravity field solutions) and of the derived topographic model in elevation. It is expected that this work will be completed well before the arrival of the MER spacecraft on Mars and that, after some appropriate verification, the MGCWG and MER missions will designate these as standard models. Thus, those solutions can be used as definitive values for the MER mission and for missions for many years into the future (until data can be obtained similar in quantity and accuracy to that obtained by the MOLA experiment).

Landing Site Local Reference System

There are several local coordinate systems defined for the spacecraft and rovers for various purposes. For the planned experiments in this paper, the Surface Fixed Coordinate System (S frame) is particularly useful. Its origin is fixed to the spacecraft. The Z axis points down in the normal direction of the Martian ellipsoid. The X axis lies on the tangent plane at the origin and points to the North Pole. The Y axis is defined such that the coordinate system is a right-handed system. The rover IMU and Sun observations can determine the relationship between the S frame and the Mars Body-fixed Reference System. Once the parameters of the S frame are computed, they remain unchanged in the operations in order to achieve

consistency, while new site-specific coordinate systems can be defined to support operations related to each site where the rover will operate. Our computations will be performed in the S frame. However, similar to the MPF mission, we will also generate topographic mapping products using the improved bundle-adjusted orientation parameters in a Landing Site Cartographic (LSC) coordinate system that is an east-north-up (*X-Y-Z*) right-handed local system (R. Kirk, personal communications, 2002). The conversion between the S frame and the LSC is a set of straightforward axis rotations. Mapping products in the LSC system are intuitive for interpretation and visualization.

Global Localization

Rover Localization through UHF Two-Way Doppler Tracking

The position of the MER rovers can be determined from measurements based on their radio systems. Each rover carries two UHF radio systems. One system is used to communicate directly with Earth tracking stations, and one is used to communicate with spacecraft orbiting Mars, including MGS and Odyssey. These spacecraft in turn relay the rover telemetry to Earth. Both radio systems allow for accurate measurement of the Doppler shift of the radio signal, from which the position of the rovers can be inferred. The radio system in communication with Earth also allows for the measurement of the range between the rovers and the Earth tracking station. From these radio measurements, the position of the rovers can be determined in the Mars inertial system within an accuracy of 1 to 10 m. It can be converted to the Mars body-fixed reference system. The accuracy of the conversion is no better than $\pm$250 m.

For communications with Earth, the rovers include an X-band radio system that receives signals sent from Earth tracking stations at a frequency of 7.2 GHz and transmits to Earth at 8.4 GHz. Earth tracking stations measure the frequency of the radio signal received from the rovers as a measure of their relative velocity with respect to Earth. In a simple one-way Doppler measurement (where the rover transmits and the Earth tracking station receives), the Doppler measurement accuracy is limited by the frequency stability of the reference oscillator on the rover, which is usually rather poor compared to the atomic frequency standards used in Earth tracking stations. In order to achieve high-quality Doppler measurements without requiring an atomic frequency standard on the rovers, the rover radio system is capable of operating in a mode where the frequency of the signal transmitted by the rover is made to be a fixed multiple of the frequency it receives from the Earth tracking station (coherent mode). In this case, the measurement of the frequency shift made by the Earth tracking station is proportional to twice the line-of-sight velocity, with a Doppler shift occurring on both the Earth-to-rover signal and on the rover-to-Earth signal. The accuracy of such measurements is generally limited by dispersion introduced by electrons in the interplanetary medium (also referred to as solar plasma). A typical frequency measurement accuracy is about 5 mHz, corresponding to a line-of-sight velocity accuracy of about 0.1 mm/s over a measurement integration time of 60 seconds (Thornton and Border, 2000).

The rover-to-Earth Doppler measurements have a time dependence due to the rotation of Mars about its axis. Measurements over a single tracking pass (view period) have a sinusoidal signature, which can be used to solve for two components of the rover position: its longitude and its distance from the Mars spin axis (Hamilton and Melbourne, 1966; Curkendall and McReynolds, 1969). As reported for the Viking and Mars Pathfinder landers (Folkner *et al.*, 1997), the Doppler measurement accuracy is sufficient to determine these components with an accuracy of about 1 m.

The third component of rover position, distance from the Mars equatorial plane, can be determined from variations in Doppler signature over multiple view periods, because the relative motion of Earth and Mars causes slight differences in signature due to Mars rotation from day to day. The accuracy with which this can be determined is quite poor over a short time period (a few months or less) because day-to-day orbital changes are fairly small. The third component of position can instead be determined by using a measurement of round-trip light time (or range) in addition to the Doppler measurements. The range measurements are made by modulating a signal onto the radio carrier frequency at the Earth tracking station and measuring the time between time of transmission and time of reception of the modulation via the rover. Range measurements are made at NASA's Deep Space Network with a typical accuracy of about 1 m. Because ranging measurements require that the rover modulate the radio signal, they can detract from transmission of telemetry (which also modulates the radio signal) and therefore are typically not available as frequently as are Doppler measurements.

The range measurements can be used in combination with Doppler measurements to determine all three components of the rover position. The third rover position component is not determined with meter-level accuracy because the range measurements depend on both the distance of the rover from the Mars equator and the distance from the center of Mars to the Earth tracking station. At the time of the Mars Pathfinder mission, the Earth-Mars distance was known within an accuracy of about 30 m, so the distance of the rover from the Mars equator was determined within an accuracy of about 80 m (Folkner *et al.*, 1997). Subsequently, knowledge of the Earth-Mars distance has been improved by about a factor of two by using a series of ranging measurements to Mars Global Surveyor and Mars Odyssey. Therefore, the MER Rover position would be expected to have an accuracy of about 40 m. Because the error in the Earth-Mars distance is nearly constant over a few sols, the range measurements can determine changes in the rover position from one sol to the next with an accuracy of about 3 m.

Due to the large distance from Mars to Earth as well as the limited antenna size and power available to the rovers, the rovers will have a radio system for transmitting data to spacecraft orbiting Mars. Because the orbiters generally have larger antennas and more power available, they can relay a much larger amount of data to Earth than could the rover if transmitting directly to Earth. The local radio signal is at UHF frequencies, with the rovers transmitting to the orbiters at 401 MHz and the orbiters transmitting to the rovers at 435 MHz. As with the X-band radio system, the rovers are capable of operating in a coherent mode with the transmitted signal referenced to the signal received by the orbiter. The Mars Odyssey orbiter uses a simple system to measure the frequency of the signal received from the rovers compared with the transmitted signal. The accuracy of the measurement is expected to be about 20 mHz, corresponding to a line-of-sight velocity accuracy of about 10 mm/s.

For each view period between the rover and the orbiter, the Doppler shift has a signature due to the relative motion between them. The signature is somewhat similar to the signature on rover-Earth signals, but with a characteristic period given by the orbiter period rather than the Mars day. The signature allows for determination of two components of the location of the rover within a single view period. Unlike the case with Earth observations, the rover-orbiter geometry changes greatly between view periods, so two consecutive tracking passes are sufficient to completely determine the rover position (assuming the rover has not moved between view periods). The rover position is determined with respect to the orbiter's position, which is typically known within an

accuracy of about 10 m through tracking of the orbiter radio signal by Earth tracking stations. The expected position determination accuracy is about 50 m (Guinn, 2001).

Rover Localization in Orbital Imagery by Triangulation

Prior to landing, the best orbital images of the landing sites will have been collected from a sequence of imaging systems, including Viking, MOC narrow angle (NA), THEMIS infrared (IRS) and visual (VIS), and possibly Mars Express High Resolution Stereo Cameras (HRSC). The individual images and possible mosaics can be registered to MOLA DIMs, which is described in the next section, and the coordinates in planetocentric latitude and east longitude of any feature visible in the images or mosaics can be estimated. The absolute accuracy of these coordinates is close to the ±100-m horizontal accuracy of the MOLA DIMs (depending on how good the tie to MOLA is). The level of precision relative to nearby features is higher (depending on the resolution and quality of the individual images or mosaics). The radius or elevation of the feature in the MOLA DIM can also be estimated from the DTM.

Within the first few sols, a complete panorama and other individual surface images may be taken by Pancam and/or Navcam. Some distinguishable landmarks at the landing site such as craters and mountain peaks will be captured by Pancam and Navcam, and may appear in the orbital images. Using the telemetry data associated with the surface imagery and the locations of the identified landmarks in both orbital and surface images, the rover location can be triangulated in an orbital image, a mosaic, or a MOLA DIM. Then its location can be transferred to any appropriate images or mosaic. The derived three-dimensional coordinates can also be assumed as initial coordinates, for example, for later bundle adjustment.

Coordinates Derived from Digital Image Models

The most straightforward way to determine the coordinates of a surface feature on Mars (or a location derivable from nearby surface features) is to locate the feature on a Digital Image Model (DIM) of Mars or possibly a MOLA shaded relief map. The radius or elevation can then be derived from the MOLA DTM. The USGS Mars Digital Image Moasics (MDIMs) with its versions of MDIM 1, color MDIM, and MDIM 2.0 (USGS, 1991; Batson and Eliason, 1995; Kirk *et al.*, 1999; Kirk *et al.*, 2000) have often been used in the past for this purpose. These MDIMs are now being superseded by higher-level MDIMs currently under development.

The MOLA topographic models (DTMs expressed as a planetocentric latitude and east longitude grid of planetary radii or elevations) may be expressed as DIMs either by creating an image color coded by height, or by illuminating the DTMs depending on applications. The primary limitations of such DIMs, however, are imposed by the horizontal resolution and sampling of the MOLA data. The footprint diameter is 168 meters, the footprint spacing along track is about 300 m, and there is about 1 to 2 km between tracks with gaps of up to 12 km at the equator (Neumann *et al.*, 2001). Therefore, in order to determine absolute coordinates of features, it is necessary either to refer to MDIMs based on the MOLA system, or to match single images or local mosaics of higher resolution images to the MOLA DIMs.

Preliminary MOLA DTMs (expressed in radii, usually with an offset value removed, or in elevation, with resolutions as fine as 1/128° horizontally) are currently available from the MOLA Science Team's Internet site, found at http://ltpwww.gsfc.nasa.gov/tharsis/mapping_data.html (last accessed 22 September 2003) where filenames containing "MEG" are in the current IAU/IAG system (Seidelmann *et al.*, 2002). It should be noted that the gridded MOLA DTMs have a uniform resolution that is lower than the MOLA footprint spacing along tracks, but higher than the across-track spacing. Despite that limited resolution, the gridded DTMs are more effective in computations. In addition, T. Duxbury (personal communication, 2002) has provided high-resolution DIMs of MOLA data at each of the proposed MER landing sites. These DIMs are currently available at ftp://naif.jpl.nasa.gov/pub/cartography/MER (last accessed 22 September 2003). Once the MOLA Science Team has completed MOLA data processing, these products will be updated to final versions that should be used for MER operational work. The primary MOLA products have been archived to the Planetary Data System (PDS) and are available at http://wufs.wustl.edu/missions/mgs/mola/ (last accessed 22 September 2003).

Additional USGS MDIMs tied to the MOLA system are in the preparation stage. These may also soon be used to obtain feature coordinates at horizontal accuracy close to that of the MOLA system, even for small features not resolved on MOLA DIMs. MDIM 2.1 (Kirk *et al.*, 1999; Kirk *et al.*, 2000) is being created by measuring tie points between Viking images and high-resolution, illuminated MOLA DIMs and then performing a new control solution of the Viking images with fixed coordinates for the MOLA tie points (Archinal *et al.*, 2002; Archinal *et al.*, 2003a; Archinal *et al.*, 2003b). This mosaic will be created by properly projecting the Viking images onto a (MOLA) topographic surface. The expected accuracy will be on the order of 250 m in the horizontal position, based on the MOLA accuracy in position (~100 m) and the ability to tie the MOLA images to those Viking images to be used in the MDIM.

Mosaics using MOC wide-angle (WA) images are now available. At Malin Space Science Systems, a 256-pixel/degree global image mosaic has been completed using MOC images mostly acquired during the "Geodesy Campaign" and some in other mapping cycles (Caplinger, 2002; see also http://www.msss.com/mgcwg, last accessed 22 September 2003). The mosaic is "uncontrolled" in that the imaging geometry is computed solely from the pointing data without any further adjustment. To improve the accuracy of the mosaic, about 100 points were selected by hand on the MOC WA images and the MOLA DTM, and then the pointing angles were adjusted manually to eliminate any systematic offset between the two data sets. The accuracy of the resultant mosaic is about 0.25 to 0.5 km when compared to the MOLA DTM (Caplinger, 2002). Experience at the USGS has shown that the pointing information is accurate, relative to MOLA-based coordinates, at less than the 1-pixel level (where 1 pixel = ~240 m in the MOC WA imagery, ~230 m in the mosaic). MDIM 3.0 is also in preparation at the USGS using MGS WA images (Kirk *et al.*, 1999). For this mosaic, it is planned to further "control" the orientation of the images by using MOLA data. This will be accomplished by incorporating pointing offsets derived from the crossover adjustment of the MOLA data, evaluated at the times of image acquisition.

Therefore, in order to determine the horizontal coordinates (planetocentric latitude and east longitude) of a surface feature at the highest level of accuracy, one must either locate it on a MOLA DIM or locate it on an image from orbit (e.g., Viking, MOC, THEMIS, or HRSC image) that is either tied to a MOLA DIM or part of a local or regional mosaic of images that is tied to a MOLA DIM. Coordinates of such features with fairly high accuracy (at the few hundred meter level in the horizontal) could alternately be obtained from MDIM 2.1 or MDIM 3.0. However, if images with higher resolution than those used in the MDIMs of the features are available (as is the case for the MER landing sites), the measurement of such features should be possible at a higher level of accuracy by doing a direct match of such images with a MOLA DIM. The absolute accuracy of any coordinates will be ultimately limited by the inherent accuracy of the MOLA system (~100 m in the horizontal) and the accuracy with which individual images can be tied to a MOLA DIM. This latter accuracy will depend primarily on how many features in the individual image in question can be matched with a MOLA DIM. For

high-resolution images (e.g., MOC NA), there may not be sufficient features present in an individual image to provide a satisfactory match or number of matches with features in a MOLA DIM. It then would be advisable to create a controlled mosaic of images (orthorectified to a MOLA DTM in order to avoid any parallax problems with oblique images), bridging the difference in resolution and area coverage of the high-resolution image(s) to the lower resolution of the MOLA DIM. The final accuracy will depend on the accuracy of the control network used to create the mosaic (how well the images of the mosaic are tied together) and on the number of tie points to the MOLA DIM (where the accuracy will improve with the square root of n, to the limit of the MOLA accuracy of ~100 m).

The situation for determining the radius or elevation of a surface feature is completely analogous. The feature must be located either on a MOLA DIM, or on an image or mosaic of images that can be tied to a MOLA DIM. If a pair of stereo images is available for the area in question, it may also be possible to establish the elevation of a feature with more precision (e.g., relative to nearby features) than that derived from a MOLA DIM. However, stereo data will not allow for any absolute improvement in the elevation (except perhaps at some minimal level by allowing for improved matching of features between the mosaic and MOLA DIM). Overall, matching of image features in both surface images and orbital images allows for the global localization of the rover in the Mars body-fixed reference system.

Rover Localization within the Landing Site

Before landing, planimetric mapping of the potential and final landing sites will be performed using orbital data such as MOLA altimetric data and images from Viking, MOC, and possibly THEMIS imaging systems by various groups such as the USGS. The first set of Pancam and/or Navcam images after landing may reveal some landmarks that can be matched with those on the orbital images. Triangulations of the matched landmarks allow for the determination of the first rover location in the global Mars body-fixed coordinate system. Independent of the success of the landmark matching technique, within three sols after landing, UHF Doppler tracking will provide rover locations in the inertial reference system at an accuracy of 30 m. The locations can be transformed to the Mars body-fixed reference system with a conversion accuracy of 250 m.

The orientation of the landing site Surface Fixed Coordinate System (S frame) can be determined by the observations of the IMU and Sun observing images within the very first few sols. Its initial origin may be determined by the above-discussed two global localization methods using radio science team observations, orbital images, and collected surface images. Although the quality of the S frame can be improved as more orbital and surface images become available, it is critical that the initially determined S frame remains consistent so that observations and computational results based on smaller areas of the landing region can be referenced to each other.

MER Onboard Rover Localization

Onboard rover position estimation for MER is done by the Surface Attitude, Position, and Pointing (SAPP) module. This module is responsible for position and attitude acquisition and propagation during the rover traverse. Position acquisition is done simply by uplinking the estimated rover position computed on Earth to the rover and is reset periodically each sol from Earth. Attitude acquisition uses onboard accelerometers to estimate rover tilt, and then uses the Pancam to find the sun. Knowledge of time and tilt are used to control the Pancam in a circular search for the sun; if this fails, then the whole hemisphere is searched. The attitude estimate resulting from this procedure is too coarse for pointing the high gain antenna (HGA), so a more accurate "sun gaze mode" is used to obtain a finer estimate for HGA pointing. In this mode, the Pancam sits still and watches the sun move across the sky for a period of about 15 minutes; the resulting observed arc produces an adequate refinement of the attitude.

Attitude propagation is done differently for nominal versus off-nominal conditions. In the nominal case, the IMU works and attitude propagation is done entirely with the IMU. The off-nominal case uses wheel odometry to propagate attitude if there is a problem with the IMU. This case updates only the rover heading, not its tilt.

Position propagation uses two different methods for the two extreme cases of nearly straight-line driving and tight turns; a weighted combination of the two methods is used for intermediate cases. In the nearly straight-line case, the method is based entirely on wheel odometry. The arc length traveled by each wheel is estimated from the wheel radius, and the wheel rotation is measured by encoders. The arc length and the steering radius for each wheel are used to estimate a turning angle for each wheel; the average over all six wheels produces a turning angle estimate for the whole rover. Basic trigonometry then gives the change in position for the rover. In the off-nominal case for attitude propagation, this also gives the change in heading for the rover. This procedure is singular when the rover is driving very nearly straight ahead; in this case, measured rotation at each wheel is used to get a displacement, and the average over all wheels produces the rover displacement. In tight turns, the gyro is used to estimate the turning angle estimate for the rover instead. There is no estimation of wheel slippage.

Both attitude and position are updated at 8 Hz while the rover is in motion. For position acquisition, a new "site frame" is defined from Earth every time a new image panorama is taken. The ground system keeps track of transformations between site frames. Science operations are commanded in the site frames. The attitude estimate has several "grades." If the grade is not "fine" before an HGA direct-to-Earth transmission, the communication behavior requests reacquisition with the sun gaze mode. The onboard localization technique provides rover locations during each sol. Updates from the ground system supply more accurate rover locations through uplinks from Earth to the rovers.

Visual odometry and bundle adjustment are two methods that were separately developed at JPL and OSU and will be experimented in this mission. The visual odometry technique is mainly for testing the potential for the "onboard" position and attitude improvement on Mars. On the other hand, the bundle adjustment technique is currently implemented for rover localization and mapping based on computations performed on Earth.

Visual Odometry

"Visual odometry" algorithms for using stereo cameras to estimate mobile robot motion were originally developed in Matthies (1989). Following this work, some minor variations and modifications were suggested for improving its robustness and accuracy (Olson *et al.*, 2000; Olson *et al.*, 2001). The key idea of this method is to determine the change in position and attitude of the rover between consecutive Hazcam image pairs acquired as the rover moves, using maximum-likelihood estimation to track point features between the images. The developed method was successfully tested at JPL and will be applied during the MER mission to provide improved initial values of orientation parameters for the bundle adjustment method.

First, features that can be easily matched in a stereo image pair and tracked over time are selected by applying an "interest operator" to one of the images. Pixels with high interest values are selected, subject to a constraint on the minimum distance between features that ensures that features are

Figure 2. The test site for visual odometry.

selected evenly across the image. Next, stereo matching is used to determine the 3D positions of the selected features.

After the rover moves a certain distance, the next pair of stereo images is acquired. The features selected from the previous pair can be projected onto one image of the new pair using prior knowledge of the approximate motion provided by the onboard wheel odometer. Then a correlation-based search and an affine template-tracking algorithm precisely determine the 2D positions of these features in the new image. The affine template tracking aims to remove the tracking error caused by large roll and scale change between images. In this case, the relationship between two images within the template is expressed as an affine transform

$$\begin{aligned} x_2 &= ax_1 + by_1 + c \\ y_2 &= dx_1 + ey_1 + f \end{aligned} \tag{1}$$

where $[a, b, c, d, e, f]$ are the unknown coefficients of the affine transform, which can be determined by iteratively minimizing the merit function (Szeliski, 1996)

$$M = \sum [I(x_1, y_1) - I(x_2, y_2)]^2 = \min. \tag{2}$$

I is image intensity. Radiometric processing of the stereo images is performed if necessary. Stereo matching is then performed to find these tracked features in the second image of the new stereo pair to determine their 3D positions relative to the new rover location. The rover motion between image pairs is estimated from the similarity transformation

$$\mathbf{Q}_{cj} = \mathbf{R}\mathbf{Q}_{pj} + \mathbf{T} + \mathbf{e}_j \tag{3}$$

where $\mathbf{R}$ is the rotation matrix and $\mathbf{T}$ is the translation vector of the rover, $\mathbf{Q}_{pj}$ and $\mathbf{Q}_{cj}$ are the positions of the observed features before and after a rover motion, and $\mathbf{e}_j$ is the combined error in the observed positions of the jth features. The variable $\mathbf{e}$ is modeled as a 3D Gaussian distribution by error propagation from the stereo triangulations that produced the estimates of $\mathbf{Q}_{pj}$ and $\mathbf{Q}_{cj}$. The three rotation angles and the translation vector $\mathbf{T}$ are estimated by minimizing the summation $\sum \mathbf{r}_j^{\mathrm{T}} \mathbf{W}_j \mathbf{r}_j = \min$, where $\mathbf{r}_j = \mathbf{Q}_{cj} - \mathbf{R}\mathbf{Q}_{pj} - \mathbf{T}$ and $\mathbf{W}_j$ is the inverse covariance matrix of $\mathbf{e}_j$. Minimization of the nonlinear problem is done by linearization and iteration (Matthies, 1989).

Visual odometry has been tested using the JPL FIDO rover (Schenker *et al.*, 2001). FIDO has two pairs of hazard avoidance stereo cameras mounted on the front and rear of the rover body about 50 cm above the ground. For each camera pair, image resolution is 640 by 480 pixels, the field of view (FOV) is 112° horizontal by 84° vertical, and the baseline is about 12 cm. The test site is a rugged, dry riverbed in the Arroyo Seco adjacent to JPL (Figure 2). FIDO experienced a lot of slip, tilting, and rolling during a test traverse that covered approximately 8 m. Images were acquired about every 20 cm of the traverse.

In order to evaluate the performance of visual odometry, high precision ground-truth data were collected with a total station survey instrument. By tracking a prism on the top of a rotating fixture, the rover's position and attitude were measured to within 3 mm in position and 0.1° in attitude. The absolute position errors at the end of this run were 2.0, 5.3, and 10.1 cm in the X, Y, and Z directions, respectively (forward, lateral, and vertical). The rotation error is less than 1.0° in general. Figures 3a and 3b show the results of this test run. While these results are quite accurate in themselves, we note that the errors in Y and Z are systematic and are correlated with the pitch and azimuth errors; hence, we think this represents the calibration error between the cameras and the rover body frame, which we expect can be improved. We are in the process of evaluating performance over a longer image sequence covering 60 m of travel in the JPL Mars Yard.

Rover Localization through Bundle Adjustment of an Integrated Image Network

The bundle adjustment method for rover localization takes a global approach by building an image network of the landing site. Starting at sol 1 after landing, the accumulated Pancam and Navcam images will be used to progressively build up an image network as the rover traverses the landing site (Figure 4). Hazcam images may be used wherever necessary to bridge the gaps in the network. Tie points that are image features appearing in the same stereo and cross-stereo image pairs of the Pancam, Navcam, and Hazcam images will be selected either automatically or manually. These tie points create a geometric configuration of the images that strengthen the geometry of the image network. The image network will expand as more surface images are acquired sol by sol.

The initial location and heading information of the rover at the times when the images are taken will be provided by the telemetry data acquired by onboard sensors and/or the improved visual odometry results. Information about the positions and pointing angles of each image, also called exterior

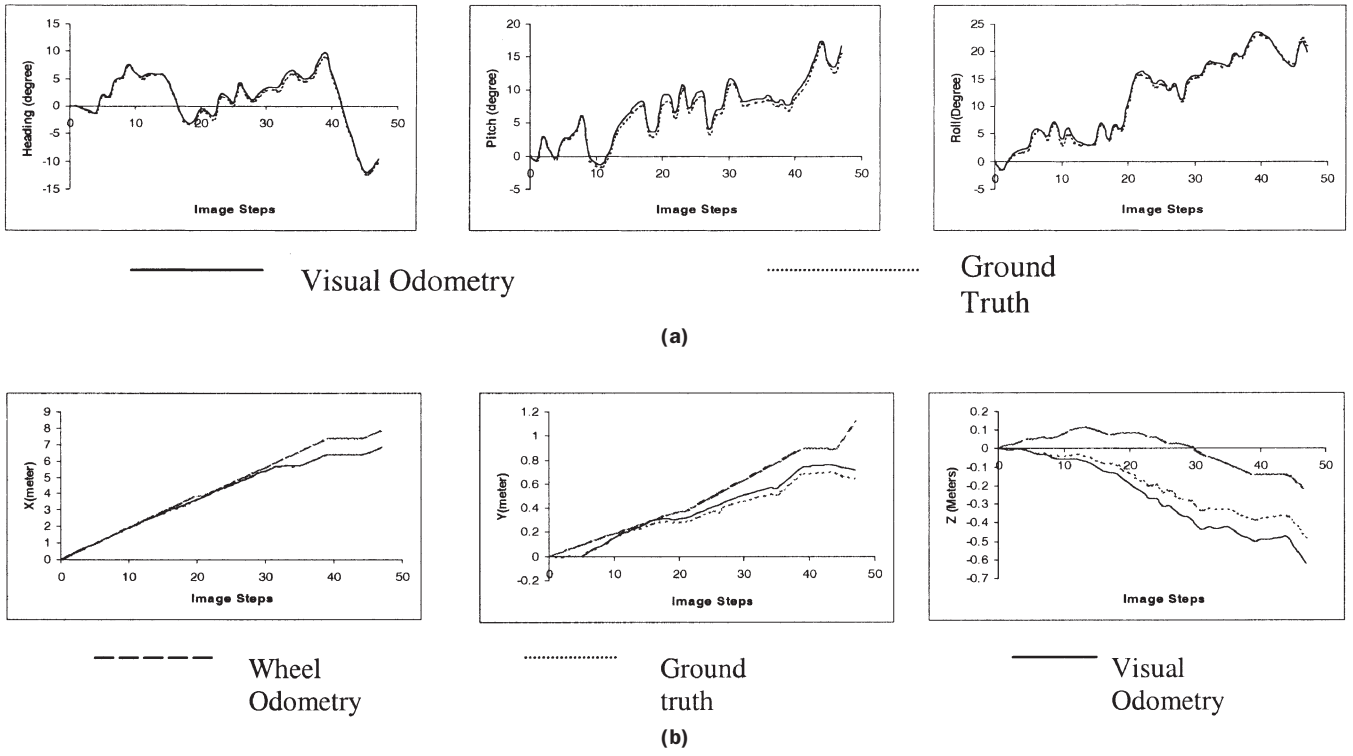

Figure 3. (a) The result of position estimation: comparisons of *X, Y,* and *Z* coordinates computed by visual odometry and ground truth. (b) The results of attitude estimation: comparisons of three attitude angles computed by wheel odometry, visual odometry, and ground truth.

orientation (EO) parameters, can also be derived. The bundle adjustment system uses the above image network to compute the refined EO parameters of all images. Because the EO parameters are estimated within the entire image network, the images are georeferenced to a high accuracy across the entire area. This is especially important for images farther away from the landing center. After the bundle adjustment, the refined EO data and Pancam and Navcam images will be employed for the generation of mapping products of the landing site, including panoramic image maps, DTM, and orthophotos.

For any image added into the image network, the bundle adjustment system can provide the camera position at the time of imaging. If locations of other rover parts (such as the rover mast, arm, or wheels) are needed, the precise location representing the rover position can also be estimated with the help of the rover calibration data (camera baseline, mast height, etc.). This bundle adjustment-based method will significantly improve rover localization capability.

We will attempt to link the MOLA altimetric data and the orbital images (including Viking, MOC NA, and THEMIS images) with the surface-based rover images in the same image network. Matches between remote landmarks in MOC NA images and IMP images of the Mars Pathfinder mission and those between a SPOT image and FIDO rover images at the FIDO field test site in Silver Lake, California, demonstrate great potential of the contribution of such remote landmarks. In a study of the optimal configuration of image networks, experimental results indicated that the remote landmarks can substantially improve the quality of orientation parameters of networked images (Di *et al.*, 2002a). This part of the work will be performed without the bundle adjustment during the mission operation. An extension of the image network to include a set of selected landmarks in both orbital and surface images for bundle adjustment will be carried out shortly after the mission operation period.

Building the Image Network

The image network consists of surface images acquired by the Pancam, Navcam, and Hazcam cameras. There should be sufficient areas of overlap between the images within stereo pairs (intra-stereo) of panoramas (Figure 4). An overlap of at least 10 percent should be maintained to facilitate the connections between adjacent stereo pairs (inter-stereo). In addition, forward- and backward-looking images are required to link the panoramas if the distances between them are significant (greater than 15 m).

The selection of tie points in image margins and overlapping areas, especially in the forward and backward images (viewing from opposite directions), is a highly challenging task. We have developed a method that can automatically designate distinct points from features such as big rocks as so-called interesting points using an interest operator such as a Förstner operator (Förstner and Guelch, 1987). Usually, there are a large number of detected interesting points. We define as candidates for the tie points those interesting points that have distinct brightness and texture, e.g., by measuring the local variance in a small window around the point. Next, image-matching techniques are employed to find the conjugate candidates of the tie points in the stereo images. The searching for matched features is constrained within a small area based on the epipolar geometry using the initial EO data. The final matched candidates are considered as the tie points. To improve the computational efficiency and to achieve an even distribution of tie points, each image is subdivided into a 3 by 3

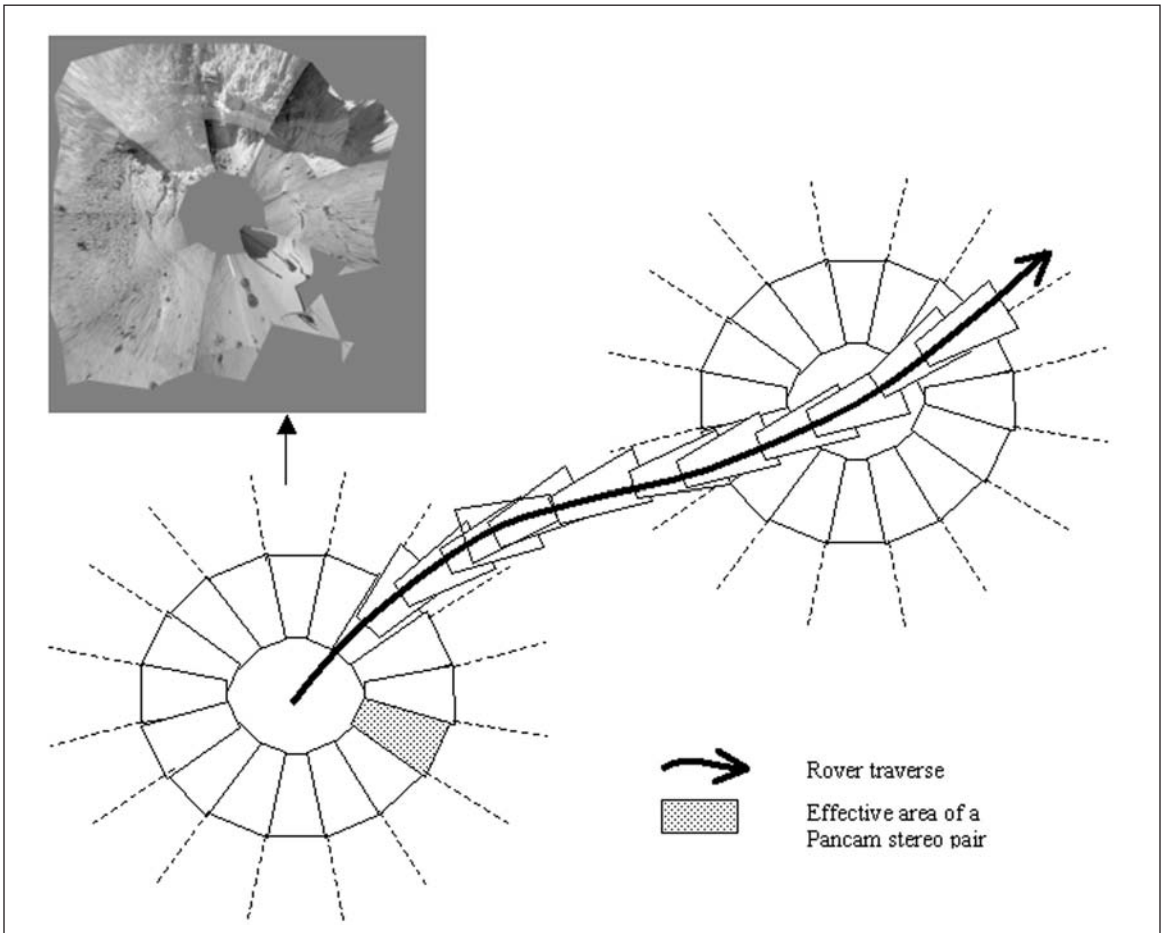

Figure 4. Illustration of a rover traverse and the network with Pancam and Navcam images.

or 5 by 5 grid. The tie point that has the highest correlation coefficient is selected within each grid. Our experiment showed that the above automatic tie-point selection techniques are capable of automatically selecting the majority of the tie points needed in panoramic images, with the remainder being chosen manually. The method is less successful in handling forward and backward traverse images (Li *et al.*, 2003).

Bundle Adjustment

The surface rover image network will be built progressively, and the bundle adjustment is conducted in an incremental manner. First, a 360° panorama of Pancam/Navcam stereo images acquired in the initial sols will be tied together to form a circular image network. This early image network will expand sol to sol as the rover collects additional images. In order to process the images and to support science and engineering operations in a timely manner, an incremental bundle adjustment will be performed for a small number of the most recently returned images (e.g., within one sol) based on the previous network adjustment result. Every few sols there will be an integrated bundle adjustment for the entire network consisting of all images collected at the landing site. This network is adjusted globally and is expected to produce the best bundle adjustment result (Li *et al.*, 2002).

An error propagation model will be developed and applied. The output of the error propagation model is a covariance matrix of all estimated unknowns, including camera positions, camera orientations, and 3D ground coordinates of the tie points. Errors associated with these unknowns can be extracted from the covariance matrix.

Achieved and Expected Results

Rover localization experiments using a FIDO rover, a helicopter-borne imaging system, and a simulated rover stereo imaging system were conducted in Silver Lake, California, in 1999 and 2000 (Arvidson and Squyres, 1999; Li *et al.*, 2000; Ma *et al.*, 2001). The developed bundle adjustment system was employed to process a set of rover images simulating the Navcam capability. In the field test of 2000, a rover traverse of 850 m with 18 rover stations (Figure 5) was established using a pair of stereo cameras (Kodak DCS 410) with a focal length of about 28.0 mm. The image size is 762 pixels by 506 pixels. At each station, the stereo cameras took forward, backward, and side-looking images. The image network consists of 76 rover images acquired at the 18 stations and it was formed from a manual selection of 217 tie points. After the bundle adjustment, accuracy of the rover locations is represented by the standard deviations of the rover positions (around 1 m). To check the external accuracy, we used 24 checkpoints that could be identified in the rover images and were measured by a differential GPS survey. Figure 6 shows the location errors (differences between the adjusted positions and known "GPS" positions) at the checkpoints. We observed a general trend that the error increases as the distance from the landing center increases. The RMS errors at checkpoints were 1.435 m, 0.883 m, and 0.752 m in the *X*, *Y*, and *Z* directions, respectively (Di *et al.*, 2002a). We also tested

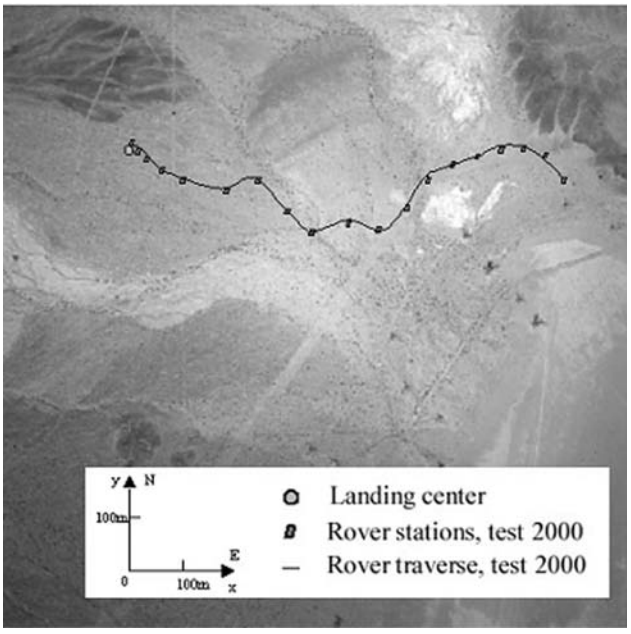

Figure 5. A traverse with rover stations of the field test in 2000.

the automatic tie point selection method. The experiment demonstrated that 262 automatically selected tie points along with a relatively small number (47) of manually selected tie points gave an accuracy similar to that of the 217 manually selected tie points.

We have tested our methods and software with actual data from the Imager for Mars Pathfinder (IMP) lander and the rover of the 1997 Mars Pathfinder mission. We selected 129 IMP images (64 stereo pairs and one single image) that form a 360° (azimuth) panorama. In the image network, there are 655 tie points, 633 of which were automatically selected and 22 were manually selected. After the bundle adjustment, image errors were reduced from tens of pixels to 0.8 pixel (Di *et al.*, 2002b; Li *et al.*, 2003). This indicates that the bundle adjustment improved the exterior orientation (EO) parameters significantly. Seamless DTM and orthoimage (Figure 7) were generated using the improved EO parameters. In addition, we selected ten stereo pairs of IMP images and two stereo pairs of rover images to test rover localization accuracy. To link the IMP images, 155 tie points were selected. Another 15 tie points were manually selected to link IMP and rover images and an additional 20 tie points were selected to link the rover images. The bundle adjustment results showed that the rover could be localized to an accuracy of about 2 percent of the distance from the lander with this lander and rover configuration. It should be noted that the rover moved in a small area and the images that can be used to build this network are limited.

The Athena Science Team conducted a FIDO field test in August 2002. In this test, the rover traversed about 200 m in 20 simulated sols, taking more than 960 Navcam and Pancam images and collecting much other data. Some of the collected Navcam and Pancam images are panoramic. We selected a 360° Navcam panorama at Site 5 to test our software. Figure 8 is a mosaic of the images. The panoramic image network is built by linking 36 Navcam images (18 pairs) with 249 automatically selected intra- and inter-stereo tie points. Before the bundle adjustment, the precision was 3.36 pixels in the image space and 0.26 meters in the object space. After bundle adjustment, the precision was 0.74 pixel in the image space and 0.10 meter in the object space. Thus, the precision was improved in both image and object space by the performed bundle adjustment. More data processing and experiments are ongoing using this data set.

Landing Site Mapping Products

Landing site mapping products will be generated by various groups involved in the mission before landing, and during and after the rover operation period as indicated in the introduction. The bundle adjustment results and the surface images can be used to generate landing site topographic mapping products with an improved accuracy.

Panoramic Maps

After the bundle adjustment, the panoramic Pancam/Navcam images are linked together by tie points in the image margins. Resampling processes will be performed in the overlapping areas of the margins to produce seamless panoramic images of the landing site. There will be one such panoramic map at

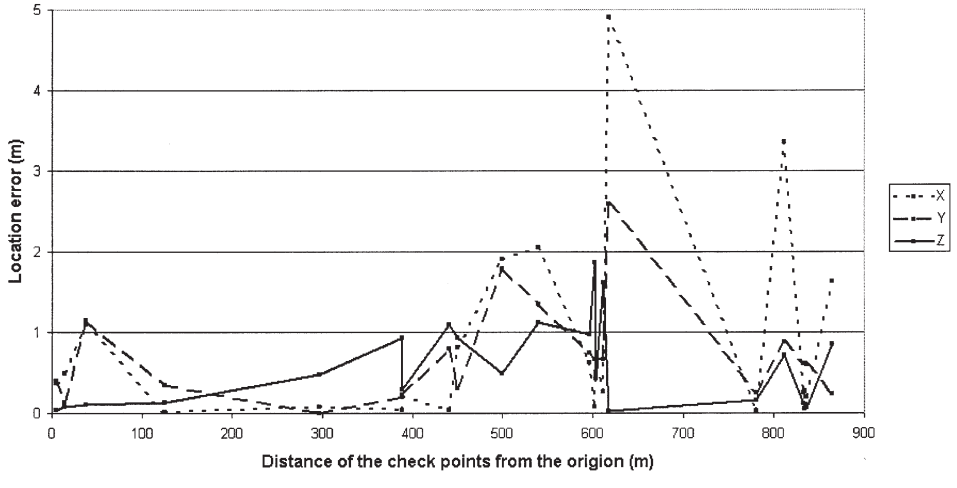

Figure 6. Location errors at check points vs. distance from the landing center.

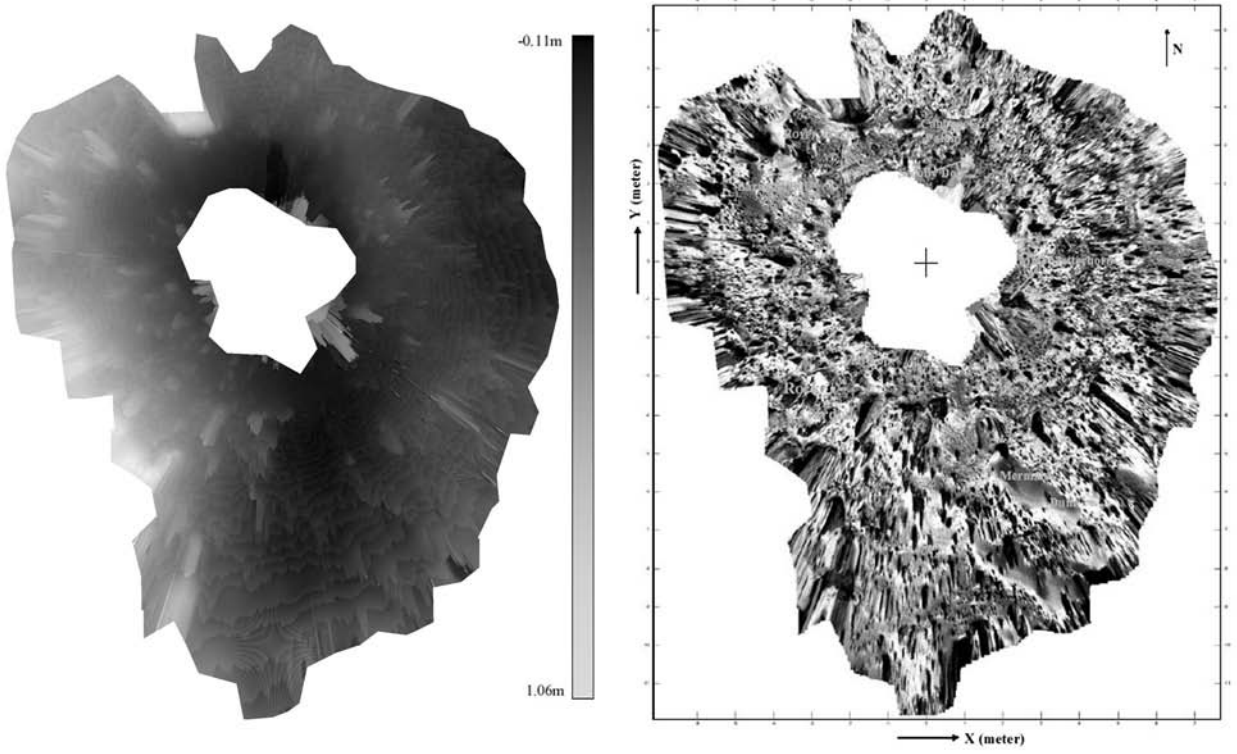

Figure 7. DTM coded in gray levels (left) and orthophoto (right) of the Mars Pathfinder landing site.

each rover site where 360° panoramic images and/or partial (less than 360°) panoramic images are taken.

Digital Terrain Model (DTM)

A detailed digital terrain model of each MER landing site will be built based on the improved orientation parameters and available Pancam, Navcam, and Hazcam images. Feature-based and area-based image matching techniques will be combined to achieve a high degree of reliability and automation in finding corresponding image features in different images. The least-squares matching technique will then be applied to improve the matching precision to a subpixel level. This is a "nonstandard" photogrammetric process for DTM generation, where (1) the resolution varies from very high in the area close to the rover to extremely low in remote regions; (2) parallaxes of remote features are very small, compared to those close to the rover; and (3) the entire site may not be covered because of obstructing terrain features such as large rocks, dunes, and small hills. In addition to the techniques discussed previously in this paper, for each matched point, we will use as many images (with different pointing angles) as possible to determine the ground location of the point. A DTM is thus established based on these ground points. The DTM can also be represented in a multi-resolution structure to match the variation of the quality and quantity of the images in different regions of the landing site. Such an improved terrain model should provide the best possible topographic information on the MER landing sites.

Orthophoto

Each MER landing site will have an orthophoto map that does not contain terrain relief distortions and that is measurable like a map. The landing site orthophotos will be produced using the improved EO parameters, the DTMs, and the Pancam,

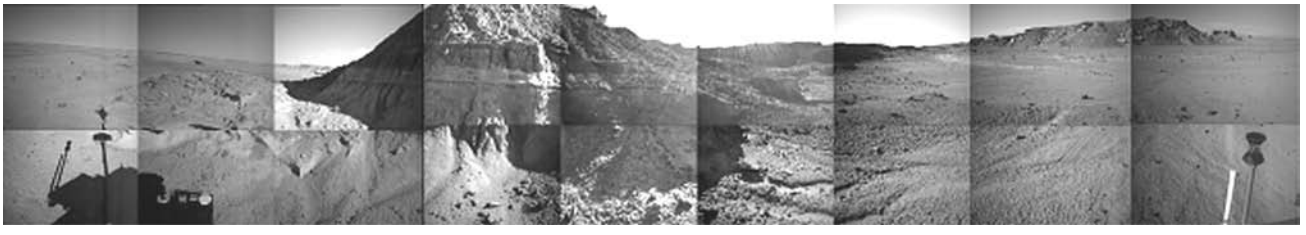

Figure 8. Mosaic of Navcam images at Site 5 of the FIDO field test in August 2002.

Navcam, and Hazcam images. Because the high quality orientation parameters are provided by the bundle adjustment, we expect very small discrepancies (subpixel) between image boundaries.

Summary

We above introduced the technology and experiments for rover localization and landing site mapping in the 2003 MER mission. At first, Mars global and landing site local reference systems will be elucidated. The initial rover position will be obtained through a triangulation using observations on orbital images and the very first set of surface images if common landmarks can be found in these images. This location can then be improved and verified by UHF two-way Doppler tracking technology. As more ground images are acquired, landmarks seen in both ground images and orbital images can be used to update landing site locations in the global Mars body-fixed reference system. Onboard rover localization techniques will perform rover localization tasks in real time. The application of visual odometry will improve localization by overcoming problems associated with wheel odometry such as slippage and low accuracy. Finally, the bundle adjustment-based rover localization method will build an image network acquired by Pancam, Navcam, and Hazcam cameras, as well as orbital images (such as Viking, MOC NA, and THEMIS images). The developed incremental and integrated bundle adjustment models will supply improved rover locations and image orientation parameters, which are critical for generation of high quality landing site topographic mapping products. Based on the field tests performed on Earth and Mars (MPF mission data), we expect that a relative localization accuracy of one percent of the traversing distance from the landing center can be achieved during this mission. In addition, the bundle adjustment results will also enable us to produce high precision landing-site topographic mapping products, including seamless panoramic image mosaics, DTM, and orthophotos.

Acknowledgments

Support from the NASA Mars Technology Program and Mars Exploration Program is appreciated. R. E. Arvidson was supported by Contract 1223696 from Cornell University as Deputy PI for the Athena Payload on the 2003 Mars Exploration Rover Mission. The research described in this paper was, in part, carried out by the Jet Propulsion Laboratory, California Institute of Technology, under a contract with NASA. We appreciate the useful comments from reviewers.

References

Archinal, B.A., T.R. Colvin, M.E. Davies, R.L. Kirk, T.C. Duxbury, E.M. Lee, D. Cook, and A.R. Gitlin, 2002. A MOLA-controlled RAND-USGS control network for Mars, *Proceedings, 33rd Lunar and Planetary Science Conference*, 11–15 March, League City, Texas (NASA Lunar and Planetary Institute, NASA Johnson Space Center, Houston, Texas), available at http://www.lpi.usra.edu/meetings/lpsc2002/lbsc2002.download.html, last accessed 06 October 2003).

Archinal, B.A., R.L. Kirk, T.C. Duxbury, E.M. Lee, R. Sucharski, and D. Cook, 2003a. Mars Digital Image Model 2.1 control network, *Proceedings, 34th Lunar and Planetary Science Conference*, 17–21 March, League City, Texas (NASA Lunar and Planetary Institute, NASA Johnson Space Flight Center, Houston, Texas), available at http://www.lpi.usra.edu/meetings/lpsc2003/lpsc2003.download.html, last accessed 06 October 2003.

———, 2003b. Mars Digital Image Model (MIDM) 2.1 control network, *Proceedings, ISPRS WG IV/9: Extraterrestrial Mapping Workshop "Advances in Planetary Mapping 2003,"* 22 March, Houston, Texas, available at http://astrogeology.usgs.gov/Projects/ISPRS/MEETINGS/Houston2003/final.html, last accessed 06 October 2003.

Arvidson, R., and S. Squyres, 1999. FIDO/APEX/ATHENA-based plans for cartographic products and rover localization Analyses, *Proceedings, ISPRS WG IV/5: Extraterrestrial Mapping Workshop "Mapping of Mars 1999,"* 23–24 July, Pasadena, California, available at http://astrogeology.usgs.gov/Projects/ISPRS/MEETINGS/Caltech99/index.html, last accessed 06 October 2003.

Batson, R.M., and E.M. Eliason, 1995. Digital maps of Mars, *Photogrammetric Engineering & Remote Sensing*, 61(12):1499–1507.

Binder, A.B., R.E. Arvidson, E.A. Guinness, K.L. Jones, E.C. Morris, T.A. Mutch, D.C. Pieri, and C. Sagan, 1977. The geology of the Viking Lander 1 site, *Journal of Geophysical Research*, 82:4439–4451.

Caplinger, M.A., 2002. Mars orbiter camera global mosaic, *Proceedings, 33rd Lunar and Planetary Science Conference*, 11–15 March, League City, Texas (NASA Lunar and Planetary Institute, NASA Johnson Space Center, Houston, Texas), available at http://www.lpi.usra.edu/meetings/lpsc2002/lpsc2002.download.html, last accessed 06 October 2003.

Crisp, J.A., M. Adler, J.R. Matijevic, S.W. Squyres, R.E. Arvidson, and D.M. Kass, 2004. The Mars Exploration Rover Mission, *Journal of Geophysical Research*, in press.

Curkendall, D.W., and S.R. McReynolds, 1969. A simplified approach for determining the information content of radio tracking data, *Journal of Spacecraft and Rockets*, 6:520–525.

de Vaucouleurs, M., E. Davies, and F.M. Sturms, Jr., 1973. The Mariner 9 Areographic Coordinate System, *Journal of Geophysical Research*, 78(20):4395–4404.

Di, K., R. Li, L.H. Matthies, and C.F. Olson, 2002a. A study on optimal design of image traverse networks for Mars Rover localization, 2002, *Proceedings, ASPRS-ACSM Annual Conference and FIG XXII Congress*, 22–26 April, Washington, D.C. (American Society for Photogrammetry and Remote Sensing, Bethesda, Maryland), unpaginated CD-ROM.

Di, K., F. Xu, R. Li, L. Matthies, and C. Olson, 2002b. High precision landing site mapping and Rover localization by integrated bundle adjustment of MPF surface images, *International Archives of the Photogrammetry, Remote Sensing and Spatial Information Sciences* (*IAPRS*), 34(4):733–737.

Duxbury, T.C., R.L. Kirk, B.A. Archinal, and G.A. Neumann, 2002. Mars Geodesy/Cartography Working Group recommendations on Mars cartographic constants and coordinate systems, *International Archives of the Photogrammetry, Remote Sensing and Spatial Information Sciences (IAPRS)*, 34(4):743–746.

Folkner, W.M., C.F. Yoder, D.N. Yuan, E.M. Standish, and R.A. Preston, 1997. Interior structure and seasonal mass redistribution of Mars from radio tracking of Mars Pathfinder, *Science*, 278(5344):1749–1752.

Förstner, W., and E. Guelch, 1987. A fast operator for detection and precise location of distinct points, corners and centers of circular features, *Proceedings, ISPRS Inter-Committee Workshop*, 02–04 June, Interlaken, Switzerland, pp. 281–305.

Golombek, M.P., 1997. The Mars Pathfinder Mission, *Journal of Geophysical Research*, 102(E2):3953–3965.

Golombek, M.P., R.C. Anderson, J.R. Barnes, J.R. Bell II, N.T. Bridges, D.T. Britt, J. Brückner, R.A. Cook, D. Crisp, J.A. Crisp, T. Economou, W.M. Folkner, R. Greeley, R.M. Haberle, R.B. Hargraves, J.A. Harris, A.F.C. Haldemann, K.E. Herkenhoff, S.F. Hviid, R. Jaumann, J.R. Johnson, P.H. Kallemeyn, H.U. Keller, R.L. Kirk, J.M. Knudsen, S. Larsen, M.T. Lemmon, M.B. Madsen, J.A. Magalhães, J.N. Maki, M.C. Malin, R.M. Manning, J. Matijevic, H.Y. McSween, Jr., H.H. Moore, S.L. Murchie, J.R. Murphy, T.J. Parker, R. Rieder, T.P. Rivellini, J.T. Schofield, A. Seiff, R.B. Singer, P.H. Smith, L.A. Soderblom, D.A. Spencer, C.R. Stoker, R. Sullivan, N. Thomas, S.W. Thurman, M.G. Tomasko, R.M. Vaughan, H. Wänke, A.W. Ward, and G.R. Wilson, 1999. Overview of the Mars Pathfinder Mission: Launch through landing, surface operations, data sets, and science results, *Journal of Geophysical Research*, 104(E4):8523–8553.

Guinn, J.R., 2001. Mars surface asset positioning using in-situ radio tracking, *Proceedings, AAS/AIAA Space Flight Mechanics Meeting*, 11–14 February, Santa Barbara, California, pp. 45–54.

Hamilton, T.W., and W.G. Melbourne, 1996. Information content of a single pass of Doppler data from distant spacecraft, *JPL Space*

Programs Summary, Jet Propulsion Laboratory, California Institute of Technology, Pasadena, California, 3(37–39):18–23.

Kirk, R., K. Becker, D. Cook, T. Hare, E. Howington-Kraus, C. Isbell, E. Lee, T. Rosanova, L. Soderblom, T. Sucharski, K. Thompson, M. Davies, T. Colvin, and T. Parker, 1999. Mars DIM: The next generation, *Proceedings, 30th Lunar and Planetary Science Conference*, 15–19 March, Houston, Texas (NASA Lunar and Planetary Institute, NASA Johnson Space Flight Center, Houston, Texas), available at http://www.lpi.usra.edu/meetings/LPSC99/download.html, last accessed 06 October 2003.

Kirk, R.L., E.M. Lee, R.M. Sucharski, J. Richie, A. Grecu, and S.K. Castro, 2000. MDIM 2.0: A revised global digital image mosaic of Mars, *Proceedings 31st Lunar and Planetary Science Conference*, 13–17 March, Houston, Texas (NASA Lunar and Planetary Institute, NASA Johnson Space Flight Center, Houston, Texas), available at http://www.lpi.usra.edu/meetings/lpsc2000/download.html, last accessed 06 October 2003.

Lemoine, F.G., D.E. Smith, D.D. Rowlands, M.T. Zuber, G.A. Neumann, D.S. Chinn, and D.E. Pavlis, 2001. An improved solution of the gravity field of Mars (GMM-2B) from Mars Global Surveyor, *Journal of Geophysical Research*, 106:23359–23376.

Li, R., F. Ma, F. Xu, L. Matthies, C. Olson, and Y. Xiong, 2000. Large scale Mars mapping and Rover localization using descent and Rover imagery, *Proceedings of ISPRS 19th Congress*, 16–23 July, Amsterdam, The Netherlands, unpaginated CD-ROM.

Li, R., F. Ma, F. Xu, L.H. Matthies, C.F. Olson, and R.E. Arvidson, 2002. Localization of Mars Rovers using descent and surface-based image data (FIDO Special Issue edited by R.E. Arvidson), *Journal of Geophysical Research-Planet*, 107(E11):FIDO 4.1–4.8.

Li, R., K. Di, and F. Xu, 2003. Automatic Mars landing site mapping using surface-based images, *Proceedings, ISPRS WG IV/9: Extraterrestrial Mapping Workshop on Advances in Planetary Mapping 2003*, 22 March, Houston, Texas, available at http://www.lpi.usra.edu/meetings/lpsc2003/lpsc2003.download.html, last accessed 06 October 2003.

Ma, C., E.F. Arias, T.M. Eubanks, A.L. Fey, A.-M. Gontier, C.S. Jacobs, O.J. Sovers, B.A. Archinal, and P. Charlot, 1998. The International Celestial Reference Frame as realized by very long baseline interferometry, *Astronomical Journal*, 116(1):516–546.

Ma, F., K. Di, R. Li, L. Matthies, and C. Olson, 2001. Incremental Mars Rover localization using decent and Rover imagery, *Proceedings, ASPRS Annual Conference*, 25–27 April, St. Louis, Missouri (American Society for Photogrammetry and Remote Sensing, Bethesda, Maryland), unpaginated CD-ROM.

Matthies, L.H., 1989. *Dynamic Stereo Vision*, PhD thesis, Carnegie Mellon University, Pittsburgh, Pennsylvania, 161 p.

Mutch, T.A., R.E. Arvidson, A.B. Binder, E.A. Guinness, and E.C. Morris, 1977. The geology of the Viking Lander 2 site, *Journal of Geophysical Research*, 82:4452–4467.

Neumann, G.A., 2002. Communication at the MGCWG (Mars Geodesy Cartography Working Group) meeting, 27 August.

Neumann, G.A., D.D. Rowlands, F.G. Lemoine, D.E. Smith, and M.T. Zuber, 2001. The crossover analysis of MOLA altimetric data, *Journal of Geophysical Research*, 106:23723–23735.

Olson, C.F., L.H. Matthies, M. Shoppers, and M. Maimone, 2000. Robust stereo ego-motion for long distance navigation, *Proceedings of the IEEE Computer Society Conference on Computer Vision and Pattern Recognition*, 13–15 June, Hilton Head Island, South Carolina, 2:453–458.

_____, 2001. Stereo ego-motion improvements for robust rover navigation, *Proceedings of the IEEE International Conference on Robotics and Automation*, 23–25 May, Seoul, Korea, pp. 1099–1104.

Oberst, J., R. Jaumann, W. Zeitler, E. Hauber, M. Kuschel, T. Parker, M. Golombek, M. Malin, and L. Soderblom, 1999. Photogrammetric analysis of horizon panoramas: The Pathfinder landing site in Viking orbiter images, *Journal of Geophysical Research*, 104(E4):8927–8933.

Schenker, P.S., E.T. Baumgartner, P.G. Backes, H. Aghazarian, L.I. Dorsky, J.S. Norris, T.L. Huntsberger, Y. Cheng, A. Trebi-Ollennu, M.S. Garrett, B.A. Kennedy, A.J. Ganino, R.E. Arvidson, and S.W. Squyres, 2001. FIDO: A field integrated design & operations rover for Mars surface exploration, *Proceedings, 6th International Symposium on Artificial Intelligence, Robotics, and Automation in Space (i-SAIRAS)*, 18–22 June, Montreal, Canada, unpaginated CD-ROM.

Seidelmann, P.K., V.K. Abalakin, M. Bursa, M.E. Davies, C. De Bergh, J.H. Lieske, J. Oberst, J.L. Simon, E.M. Standish, P. Stooke, and P.C. Thomas, 2002. Report of the IAU/IAG Working Group on Cartographic Coordinates and Rotational Elements of the Planets and Satellites: 2000, *Celestial Mechanics and Dynamical Astronomy*, 82(1):83–110.

Smith, D.E., M.T. Zuber, H.V. Frey, J.B. Garvin, J.W. Head, D.O. Muhleman, G.H. Pettengill, R.J. Phillips, S.C. Solomon, H.J. Zwally, W.B. Banerdt, T.C. Duxbury, M.P. Golombek, F.G. Lemoine, G.A. Neumann, D.D. Rowlands, O. Aharonson, P.G. Ford, A.B. Ivanov, P.J. Mcgovern, J.B. Abshire, R.S. Afzal, and X. Sun, 2001. Mars Orbiter Laser Altimeter: Experiment summary after the first year of global mapping of Mars, *Journal of Geophysical Research*, 106:23689–23722.

Squyres, S.W., R.E. Arvidson, E.T. Baumgartner, J.F. Bell III, P.R. Christensen, S. Gorevan, K.E. Herkenhoff, and G. Klingelhöfer, 2004. The Athena Mars Rover Science Investigation, *Journal of Geophysical Research*, in press.

Szeliski, R., 1996. Video mosaics for virtual environments, *IEEE Computer Graphics and Applications*, 16(2):22–30.

Thornton, C.L., and J.S. Border, 2000. *Radiometric Tracking Techniques for Deep Space Navigation*, Monograph 1, Deep Space Communications and Navigation Series, Jet Propulsion Laboratory, California Institute of Technology, Pasadena, California, 85 p.

U.S. Geological Survey, 1991. *Mission to Mars: Digital Image Maps*, PDS Volumes USA_NASA_PDS_ VO_2001 through VO_2007, U.S. Geological Survey, Reston, Virginia, CD-ROM.

Wu, S., 1975. *Topographic Mapping of Mars*, Interagency Report: Astrogeology 63, U.S. Geological Survey, Reston, Virginia.

(Received 14 January 2003; accepted 27 August 2003; revised 04 September 2003)